We appreciate 4th referee for highlighting the significant questions which help us to clarify the main results of research.

1. *It should be stressed in the manuscript that the 3-wave system analysis can only be relevant at the initial stages of evolution, as long as the sidebands are sufficiently small and thus no significant new harmonics are generated due to nonlinear near-resonant interactions. It is well known that addition of even a single new harmonic to an initially 3 wave system prevents exact Fermi-Pasta-Ulam recurrence. The FPU recurrence thus cannot be expected to occur in reality. Nevertheless, this simplified wave system may be useful if reservations regarding the limited validity of results are understood and clearly spelled out.*

The evolution of the wave spectrum in the absence of breaking includes energy exchange between the carrier wave and two main resonant side-bands and spreading of the energy to higher frequencies. Inclusion of higher frequency free waves in the Zakharov, modified Schrodinger or Dythe equations is crucial, since the asymmetry of the lower and the upper side-band amplitudes at peak modulation in non-breaking case results from that. Such a conclusion can be made regarding to developing of modulation instability in a calm water.

The developing of modulation instability in the presence of significant adverse current is different. Experimental results of Chavla and Kirby (2002) and Ma et al. (2010) clearly show that energy spectrum is mostly concentrated in the main triad of waves and high frequency discretized energy spreading is depressed due to the short wave blocking by the strong enough adverse current.

The relatively high initial wave steepness leads to wave breaking dissipation with discriminatory energy loss from the carrier and higher side-band modes (Tulin and Waseda, 1999). Even those waves which do not blocked lose a considerable amount of energy due to wave breaking on the strong opposite current. The permanent frequency downshift with final dominating of the lower subharmonic takes a place and wave system does not revert to its initial state.

3-wave dynamical model analysis in the presence of significant opposite current therefore can be relevant not only at the initial stages but also at the further stages of wave evolution.

Corresponding discussion added to text of paper.

2. *As mentioned by the 2nd reviewer, the evolution of the 3-wave system beyond the initial exponential growth stage has been considered before. The main motivation for limiting the analysis to 3 waves only in those works was the availability of a closed analytical solution in the framework of the Zakharov equation (see the book by Mei et al., Stiassnie and Shemer 1987, 2005 and Shemer 2009). The possibility to apply similar analytical approach in the presence of the current should be examined and discussed in the paper. The current investigation considers spatial evolution, whereas the temporal variation was apparently studied in the earlier publications mentioned above. The advantages (if any) of the adopted approach also have to be discussed. The present formulation has the 3rd order accuracy and thus should not be essentially different from the Zakharov equation (at least in the absence of the current). The differences between the two formulations have to be clarified and an effort made to carry out quantitative comparison of results when possible.*

The obtained system of equations (20) in the absence of current is similar to classical Zakharov equations for discrete wave interactions (Mei, You and Stiassnie, 2009 . Theory and Applications of Ocean Surface Waves. World Scientific, 2009, 14.9.1-14.9.3). Corresponding references are added to the text.

Following reviewer recommendations we rewrite equations (17), (20) in a more clear and compact form of wave action law:

$$\begin{cases} [\phi_0^2\sigma_0]_T + [(U(X)+\dfrac{1}{2\sigma_0})\phi_0^2\sigma_0]_X = \varepsilon\phi_1^2\phi_2\phi_0\sigma_1^3\sigma_2^2(2\sigma_1^3 \text{-} 2\sigma_1^2\sigma_2 + 2\ \sigma_1\sigma_2^2 \text{-} \sigma_2^3)\ \mathrm{Sin}[\varphi]; \\[2mm] [\phi_2^2\sigma_2]_T + [(U(X)+\dfrac{1}{2\sigma_2})\phi_2^2\sigma_2]_X = \varepsilon\phi_1^2\phi_2\phi_0\sigma_0^2\sigma_1^3(2\sigma_1^3 \text{-} 2\sigma_0\sigma_1^2 + 2\sigma_0^2\sigma_1 \text{-} \sigma_0^3)\ \mathrm{Sin}[\varphi]; \\[2mm] [\phi_1^2\sigma_1]_T + [(U(X)+\dfrac{1}{2\sigma_1})\phi_1^2\sigma_1]_X = -\varepsilon\phi_1^2\phi_2\phi_0\sigma_0\sigma_1^2\sigma_2(\sigma_0^4 - \sigma_0^3\sigma_1 - \sigma_0\sigma_1(\sigma_1-\sigma_2)^2 + \\[2mm] +\sigma_0^2(\sigma_1^2\text{-}\sigma_1\sigma_2+2\sigma_2^2)\text{-}\sigma_2(\sigma_1^3\text{-}\sigma_1^2\sigma_2+\sigma_1\sigma_2^2\text{-}\sigma_2^3))\mathrm{Sin}[\varphi]; \end{cases} \tag{17}$$

$$\begin{cases} [(U+\dfrac{1}{2\sigma_0})\phi_0^2\sigma_0]_X = \varepsilon\phi_1^2\phi_2\phi_0\sigma_1^3\sigma_2^2(2\sigma_1^3\text{-}2\sigma_1^2\sigma_2 + 2\ \sigma_1\sigma_2^2\text{-}\sigma_2^3)\ \mathrm{Sin}[\varphi] \\[2mm] [(U+\dfrac{1}{2\sigma_2})\phi_2^2\sigma_2]_X = \varepsilon\phi_1^2\phi_2\phi_0\sigma_1^3\sigma_0^2(2\sigma_1^3\text{-}2\sigma_0\sigma_1^2 + 2\sigma_0^2\sigma_1\text{-}\sigma_0^3)\ \mathrm{Sin}[\varphi] \\[2mm] [(U+\dfrac{1}{2\sigma_1})\phi_1^2\sigma_1]_X = -\varepsilon\phi_1^2\phi_2\phi_0\sigma_0\sigma_1^2\sigma_2(\sigma_0^4 - \sigma_0^3\sigma_1 - \sigma_0\sigma_1(\sigma_1-\sigma_2)^2 + \\[2mm] \sigma_0^2(\sigma_1^2\text{-}\sigma_1\sigma_2+2\sigma_2^2)\text{-}\sigma_2(\sigma_1^3\text{-}\sigma_1^2\sigma_2+\sigma_1\sigma_2^2\text{-}\sigma_2^3))\mathrm{Sin}[\varphi] \end{cases} \tag{20}$$

The main property of the derived modulation equations is the variability of interaction coefficients in the presence of variable current.

To perform the qualitative analysis of the stationary problem, we suggest the law of wave action conservation flux in a slowly moving media as analogue of the three Manley-Rowe dependent integrals:

$$\begin{cases} \left(U+\dfrac{1}{2\sigma_2}\right)\phi_2^2\sigma_2 + \left(U+\dfrac{1}{2\sigma_0}\right)\phi_0^2\sigma_0 + \left(U+\dfrac{1}{2\sigma_1}\right)\phi_1^2\sigma_1 = const; \\[3mm] \dfrac{1}{2}\left(U+\dfrac{1}{2\sigma_1}\right)\phi_1^2\sigma_1 + \left(U+\dfrac{1}{2\sigma_0}\right)\phi_0^2\sigma_0 = const; \\[3mm] \dfrac{1}{2}\left(U+\dfrac{1}{2\sigma_1}\right)\phi_1^2\sigma_1 + \left(U+\dfrac{1}{2\sigma_2}\right)\phi_2^2\sigma_2 = const; \\[3mm] \left(U+\dfrac{1}{2\sigma_0}\right)\phi_0^2\sigma_0 - \left(U+\dfrac{1}{2\sigma_2}\right)\phi_2^2\sigma_2 = const. \end{cases}$$

These integrals follow from the system (20) with acceptable accuracy $O(\varepsilon^4)$ for the stationary regime of modulation. The second and third relations here clearly show that the wave action flux of the side bands can grow up at the expense of the main carrier wave flux. The last relationship manifests the almost identical behavior of the main sidebands for the problem of their generation due to Benjamin-Feir instability.

3. *The manuscript is prepared quite sloppily and some references (for example, Moreira and Peregrine, among others, or Hwung et al 2010) do not appear in the list.*

Reference list is checked and updated.

R. M. Moreira and D. H. Peregrine. (2012) Nonlinear interactions between deep-water waves and currents
Journal of Fluid Mechanics, Vol. 691, pp 1- 25.

W. Chiang, H. Hwung (2012) Large transient waves generated through modulational instability in deep water
Journal of Hydrodynamics, 22(5), pp. 114-119. DOI: 10.1016/S1001-6058(09)60179-7

4. *I failed to understand the small slope approximation on line 15 p. 1811.*

Small slope approximation follows from the stationary shallow water model for a large scale slowly varying current.

IV - th assumption of the model is rewritten.

5. *The initial conditions in the simulations are not defined. As follows from the previous studies, the evolution pattern strongly depends not only on the frequencies of the sidebands, but also on their initial amplitudes and phases. I found no mention of these quantities in the manuscript, and subsequently there is no attempt to discuss their relative importance.*

The development of side band instability highly depends from amplitudes and phases of initially imposed side bands. Increasing of initial amplitudes of side bands sharply accelerate the instability. Initial phase shift between side bands and carrier in our simulations was always taken to $-\pi/4$ corresponding to the maximum growth condition predicted by Benjamin & Feir (1967).

Boundary conditions for sideband amplitudes and phases are specified in the text.

6. *The dissipation due to breaking is introduced into the model equation. The parameters used are not specified, and the important details of the dissipation model used in the simulations are missing. Moreover, I question the importance of dissipation in the framework of this study. The variation of the amplitude of various harmonics in the spectrum in the process of breaking was studied in some recent studies (see, e.g. Perlin et al. Ann. Rev. Fluid Mech. 2013 and references therein) and was found to be hardly detectable. As the details of the dissipation model are missing, it remains unclear to what extent accounting for dissipation in the present work indeed affects the results. On the other hand, even prior to breaking the 3-wave approximation adopted in the study apparently ceases to be even approximately valid, as new harmonics inevitably emerge due to nonlinearity. This phenomenon most probably is much more significant than dissipation. It would be highly desirable to have some spectral information from experiments about the wave field, both as initially generated and at advanced stages of evolution. In any case, the relative significance of various factors that lead to poor agreement with available measurements has to be discussed.*

We employ the adjusted dissipative model of Tulin and Li (1996) and Huang et al. (2011) to describe the effect of breaking on the dynamics of the water wave. The sinks of energy and momentum terms for each of the waves are calculated in accordance with the dissipative Schrodinger model for the complex amplitude $A \sim \sum_i \phi_i e^{i\theta_i}$ ::

$$A_T + C_g A_X + i \frac{C_g}{4k} A_{XX} + \frac{i}{2}\omega k^2 |A|^2 A = \left(-\frac{DA}{g|A|^2} - 4i\gamma A \int \frac{\omega^2 D dX}{g|A|^2} \right) H\left[\frac{|A_X|}{A_S} - 1 \right]$$

where $D \sim gD_b|A|^4, D_b = O(10^{-1}), \gamma = O(10^{-1})$ - constants of proportionality taken from the field observations, g – gravity acceleration, H is the Heaviside unit step function, and A_S is the threshold value of the characteristic steepness $A_X = \varepsilon \sum \sigma_i \phi_i k_i$. Right side part leads to additional terms in the governing modulation equations (16), (17), (20).

Wave breaking leads to permanent (not temporal) frequency downshifting at a rate controlled by breaking process. A crucial aspect here is the cooperation of dissipation and near-neighbor energy transfer in the discretized spectrum acting together.

We add some more figures with additional examples of wave interactions accompanied by breaking dissipation to clarify its properties.

The numerical simulations for initially high steepness waves ($\varepsilon = 0.25$) propagation with wave breaking dissipation is

presented in Fig. 3(a-c). We calculate the amplitudes of surface waves on linearly increasing opposing current $U(x) = -U_0 x$ with different strength U_0. Most unstable regime was tested for frequency space $\Delta\omega_\pm / \omega_1 \sim \varepsilon$ and most effective initial phases $\theta_1(0) = 0, \theta_0(0) = \theta_2(0) = -\pi/4$
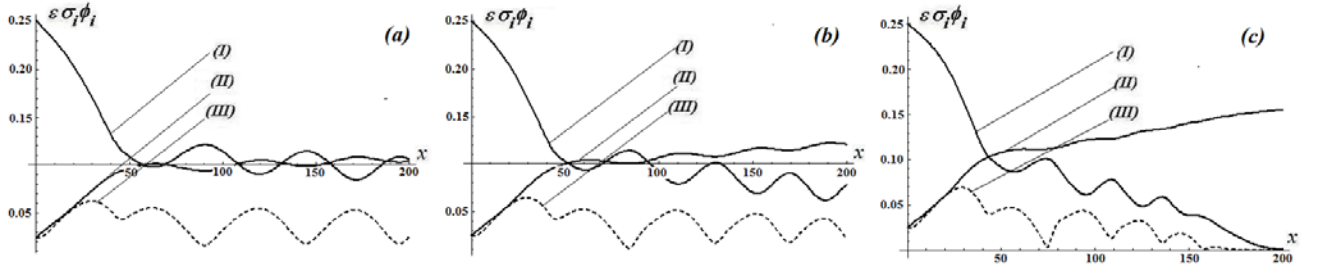

FIG. 3. Modulation of surface waves by the adverse current $U = U_0 x$. (a) $U_0 = -2.5\ 10^{-4}$; (b) $U_0 = -5\ 10^{-4}$, (c) $U_0 = -10^{-3}$. (I), (II), (III) - amplitude envelopes of the carrier, subharmonic and superharmonic waves, respectively. Initial wave steepness $\varepsilon = 0.25$. Dissipation parameters $D_b = 0.1, \gamma = 0.5$

A very weak opposite current $U_0 = 2.5\ 10^{-4}$ (Fig.3(a)) has a pure impact on wave behavior: it is finally results in almost bichromatic wave train with two dominant waves: carrier and lower side band. Frequency downshift here is not clearly seen. Two times stronger current case with $U_0 = 5\ 10^{-4}$ is presented in Fig. 3(b). We note some tendency to final energy downshift to the lower side band. Really strong permanent downshift with total domination of the lower side band is seen for two times more strong current $U_0 = 10^{-3}$.